Multicenter Study of Quantitative SPECT: Reproducibility of ^{99m}Tc Quantitation Using a Conjugated-Gradient Minimization Reconstruction Algorithm

Kyohei Okuda[1], Daisuke Hasegawa[2], Takashi Kamiya[3], Hajime Ichikawa[4], Takuro Umeda[5], Takushi Ohkubo[6], and Kenta Miwa[7]

[1]Department of Clinical Radiology, Tottori University Hospital, Yonago, Japan; [2]Department of Radiology, Okayama Saiseikai General Hospital, Okayama, Japan; [3]Division of Radiology, Department of Medical Technology, Osaka University Hospital, Suita, Japan; [4]Department of Radiology, Toyohashi Municipal Hospital, Toyohashi, Japan; [5]Department of Nuclear Medicine, Cancer Institution Hospital of Japan Foundation for Cancer Research, Tokyo, Japan; [6]Central Division of Radiology, Toho University Omori Medical Center, Tokyo, Japan; and [7]School of Health Science, International University of Health and Welfare, Ohtawara, Japan

This multicenter study aimed to determine the reproducibility of quantitative SPECT images reconstructed using a commercially available method of ordered-subset conjugate-gradient minimization. **Methods:** A common cylindric phantom containing a 100 kBq/mL concentration of ^{99m}Tc-pertechnetate solution in a volume of 7 L was scanned under standard imaging conditions at 6 institutions using the local clinical protocol of each. Interinstitutional variation among the quantitative SPECT images was evaluated using the coefficient of variation. Dose calibrator accuracy was also investigated by measuring the same lot of commercially available ^{99m}Tc vials at each institution. **Results:** The respective radioactivity concentrations under standard and clinical conditions ranged from 95.71 ± 0.60 (mean ± SD) to 108.35 ± 0.36 kBq/mL and from 96.78 ± 0.64 to 108.49 ± 0.11 kBq/mL, respectively. Interinstitutional variation in radioactivity concentration was 4.20%. The bias in the radioactivity concentrations in SPECT images was associated with the accuracy of the dose calibrator at each institution. **Conclusion:** The reproducibility of the commercially available quantitative SPECT reconstruction method is high and comparable to that of PET, for comparatively large (~7 L), homogeneous objects.

Key Words: SPECT/CT; OSCGM; quantification; dose calibrator; ^{99m}Tc-MDP

J Nucl Med Technol 2021; 49:138–142
DOI: 10.2967/jnmt.120.256131

SPECT imaging has been considered less quantitatively accurate than PET because of issues with sensitivity, spatial resolution, and various corrections, including photon attenuation and scatter (*1–4*). The recent introduction of hybrid SPECT devices equipped with CT capability has allowed not only lesion localization but also more accurate quantitative assessment by correcting image-degradation factors (*1,5*). Several studies have suggested that the SUV in SPECT/CT images is sufficiently accurate to have clinical value (*1,5–13*), and Bailey et al. (*1*) reported that SPECT/CT quantitative accuracy is comparable to that of PET/CT.

Siemens Healthcare introduced the xSPECT Quant reconstruction engine to apply SPECT quantitation to clinical practice (*14,15*). For accuracy, xSPECT Quant uses the CT coordinate system to improve alignment between SPECT and CT images. The change in image-formation space from a SPECT image to a CT image increases data volumes and prolongs calculation time. To address this change, xSPECT Quant uses a unique algorithm, namely ordered-subset conjugate-gradient minimization (OSCGM), which has faster convergence than conventional ordered-subset expectation maximization. The projection data are processed as count rates in OSCGM reconstruction. This concept differs from conventional count-based SPECT reconstruction and is similar to PET, with voxel units of Bq/mL. Moreover, by calibrating the scanner to a reference source, xSPECT Quant reconstructs SPECT voxels in units of Bq/mL. Calibration is performed

TABLE 1
Details of System Sensitivity Calibration at Participating Institutions

Institution	Calibration source	SCF ($s^{-1}MBq^{-1}$)	
		Detector 1	Detector 2
A	^{99m}Tc	86.8	88.1
B	^{57}Co	88.2	88.7
C	^{99m}Tc	87.6	84.9
D	^{99m}Tc	89.9	85.3
E	^{57}Co	90.1	89.1
F	^{99m}Tc	87.7	88.2

Received Sep. 17, 2020; revision accepted Jan. 3, 2021.
For correspondence or reprints contact: Kyohei Okuda, Department of Clinical Radiology, Tottori University Hospital, 36-1 Nishi-cho, Yonago, Tottori 683-8504, Japan.
E-mail: kokuda-jsnmt@umin.ac.jp
Published online Jan. 8, 2021.

once every 30 d using a ^{57}Co standard point source (or ^{99m}Tc) to maintain quantitative accuracy. Kuji et al. reported that the quantitative indices generated by xSPECT Quant are helpful for bone SPECT/CT (*16*). According to previous studies that used a uniform phantom, the quantitative accuracy of xSPECT Quant is 3%–6% (*17*). The clinical value and quantitative accuracy of xSPECT Quant have been reported as above, but reproducibility at several institutions has not yet been reported, to our knowledge. The present multicenter study aimed to determine this reproducibility. To determine whether there is any interinstitutional bias associated with the radioactivity measurements, the accuracy of the dose calibrator at each institution was also evaluated.

MATERIALS AND METHODS

Participating Institutions

The Symbia Intevo (Siemens Medical Solutions USA Inc.) SPECT/CT system with xSPECT Quant was installed at the 6 institutions (institutions A–F) that participated in the present phantom study. Table 1 summarizes the calibration sources and the sensitivity calibration factors (SCFs) used at these institutions during phantom image acquisition. Two institutions measured the SCF using a ^{57}Co standard point source within 3% National Institute of Standards and Technology–traceable accuracy. Others used ^{99m}Tc point sources created in house, whose radioactivity were measured with the individual dose calibrator certified by each manufacturer within a year for the SCF measurements.

Phantom Measurements

A uniform cylindric phantom with a diameter of 21 cm (volume, 6,810 mL) was set up by removing all the internal features (cold spheres and cold rods) of a Jaszczak phantom (Data Spectrum Corp.) and was scanned at each institution. The concentrations of aqueous ^{99m}Tc solution in the phantoms were adjusted to 100 kBq/mL using the dose calibrator at each institution, with the pure water volume determined according to the measured radioactivity (~800 MBq). We used a graduated cylinder with a total volume of 1,000 mL and accuracy of 2.0 mL to adjust solution volumes. SPECT scans were started immediately after phantom filling. To standardize the radioactive concentration of the output images, the radioactive decay of ^{99m}Tc, from the radioactivity measurement with dose calibrator to the SPECT scan, was corrected in the SPECT reconstruction process. The unit of the output images mean the radioactive concentration at the time of the ^{99m}Tc measurement by each dose calibrator. We conducted tests under 2 imaging conditions. First, standardized study conditions were created to minimize variables when acquiring phantom imaging data at each site. Then, the routine acquisition and reconstruction conditions for bone SPECT imaging at each institution were adopted to assess potential interinstitutional variability in daily clinical practice. Under the standardized study conditions, the images were acquired using a low-energy high-resolution collimator, a 256 × 256 matrix, and a 2.4-mm pixel size. The energy window setting for ^{99m}Tc was 129.5–150.5 keV, and the scatter window setting was 108.5–129.5 keV. The cylindric phantom was carefully located at the center of the field of view using CT positioning lasers. Phantom images were acquired from 72 projections over a 360° circular orbit with step-and-shoot mode, and the rotation radius of the detector was 260 mm. The time taken for each projection was adjusted to 20 s, corresponding to a total acquisition duration of 12 min. CT images were then acquired using 130 keV, 50 mA, a tube rotation duration of 0.6 s, and a pitch of 1.0. The CT data were reconstructed with a slice thickness of 2.0 mm and a display field of view of 500 mm. Under the clinical conditions, the modes of acquisition, projection numbers, and amount of time per view varied among institutions (Table 2). The CT acquisition parameters were not standardized, and interinstitutional variability existed with respect to mA, slice thickness, and field-ofview settings. Images were reconstructed using the OSCGM algorithm, integrating scatter correction with energy window–based scatter estimation and attenuation correction according to an attenuation map derived from the CT data. The scatter estimation is modeled in OSCGM as part of the forward-projection step in the reconstruction iteration. Details on OSCGM reconstruction have been described elsewhere (*14*,*15*). Under the standardized study conditions, the OSCGM reconstruction was set to 30 iterations per subset, as based on the previous study (*17*), to optimize balance between the convergence for accurate quantification and the degradation of image uniformity. A gaussian filter with a full width at half maximum of 6 mm was used for postacquisition smoothing. Table 2 shows that these reconstruction parameters varied among the institutions under the clinical conditions. To assess further variabilities introduced by differences in clinical routine, an optional reconstruction application adapted for bone SPECT, namely xSPECT Bone, was used at institutions A, C, E, and F. All reconstructed data units were generated in Bq/mL using the SCF measured at each institution. Intrainstitutional reproducibility was examined at institution A, in which 2 Symbia Intevo SPECT/CT systems were installed. To get 6 datasets from 1 institution to complement the 6 datasets from 6 institutions, phantom filling and data acquisition were repeated 3 times on separate days for each of the 2 systems.

Dose Calibrator Accuracy

The accuracy of the dose calibrators was investigated using a commercially available ^{99m}Tc source; its manufacturer (NihonMedi- Physics Co. Ltd.) delivered the same lot number to each institution. Because the manufacturer's dose calibrator is certified regularly with National Institute of Standards and Technology–traceable standards, it was assumed that variations in the radioactivity and volume of the ^{99m}Tc solution in the same lot were negligible, and we defined the operational true activity in the reference source as the value measured at the manufacturer's factory (410.6 MBq in 1.13 mL at the assay date and time, with variation of 62%). The diameter of each glass vial containing ^{99m}Tc solution was 17.0 mm. The ^{99m}Tc vial was measured at 5 time points over 3 d, with the theoretic activity ranging from 615 to 2 MBq, using a dose calibrator available at each institution. To minimize background radioactivity, each measurement was taken in an environment that had no other radioactive sources or radiowave-emitting devices, after the dose calibrators had been warmed up.

Data Analysis

All SPECT images, acquired and reconstructed at the individual institutions, were transferred to the central institution (Tottori University Hospital) in DICOM format and analyzed using the OsiriX DICOM viewer, version 5.6 (Pixmeo). The mean radioactivity concentration (kBq/mL) in 5 circular regions of interest, drawn on consecutive slices in the center of the cylinder phantom, was calculated. Each region of interest encompassed about 80% of the interior diameter of the phantom (Fig. 1). The results were expressed as mean 6 SD. We evaluated reproducibility as the interinstitutional variation in radioactivity concentrations in SPECT images, calculated using the following formula:

TABLE 2
Bone SPECT Image Acquisition and Reconstruction Conditions Used for Clinical Conditions at Participating Institutions

Institution	Acquisition			Reconstruction	
	Mode	Number of projections	Duration of projection (s)	Updates	Gaussian filter (full width at half maximum; mm)
A	Continuous	90	12	48 (2 subsets)	5
B	Step and shoot	120	10	30 (1 subset)	6
C	Continuous	90	12	48 (2 subsets)	10
D	Continuous	120	9	30 (1 subset)	7
E	Step and shoot	72	20	48 (2 subsets)	5
F	Continuous	72	16	40 (1 subset)	7

$$\text{Variation}\,(\%) = \text{SD}/\text{mean} \times 100,$$

where mean represents the mean radioactivity concentration of acquired SPECT images and SD represents the SD of the radioactivity concentrations of the participating institutions.

Measurement accuracy in the dose calibrator test was calculated as the difference in radioactivity from the reference value as follows:

$$\text{Accuracy}\,(\%) = \left(A_{\text{meas}}/A_{\text{ref}} - 1\right) \times 100,$$

where A_{meas} is the activity measured at each of the participating institutions and A_{ref} is the activity measured at the manufacturer's factory (410.6 MBq at the assay date and time).

Statistical Analysis

Differences in reproducibility were compared between the 2 imaging conditions using Wilcoxon signed-rank tests and *F* tests. *P* values of less than 0.05 were considered to indicate a statistically significant difference. All data were statistically analyzed using MATLAB, version R2013a (The MathWorks Inc.).

RESULTS

The radioactivity concentrations in SPECT images acquired under the standardized and clinical conditions were 95.71 ± 0.60 to 108.35 ± 0.36 and 96.78 ± 0.64 to 108.49 ± 0.11 kBq/mL, respectively (Table 3). Interinstitutional variation under these 2 conditions was, respectively, 4.20% and 3.89%. Reproducibility did not significantly differ between the 2 imaging conditions ($P = 0.394$, Wilcoxon signed-rank test; $P = 0.893$, *F* test). The results of the intrainstitutional examination at institution A are summarized in Table 4. The radioactivity concentrations in SPECT images acquired under the standardized conditions, as tested with the 2 scanners repeatedly, were 98.96 ± 0.07 to 101.81 ± 0.30 kBq/mL.

In Table 5, we show that at most institutions, the measurement accuracy of the dose calibrators was within ±5% of the manufacturer's measurement. However, the measurement error at institution F was relatively high (6.13% ± 0.44%). The measured values at institutions A, B, C, D, and F tended to be higher than the reference value, whereas the measured value at institution E was an underestimation.

DISCUSSION

Quantitative SPECT images can be generated using a commercially available OSCGM application, xSPECT Quant, the clinical use of which is becoming more prevalent. The present multicenter study investigated the reproducibility of quantitative SPECT images generated using this application. The interinstitutional variation in radioactivity concentrations was 4% under the 2 study conditions. PET studies have been reported to show a similar level of variability (*18*), suggesting that the quantitative reproducibility of xSPECT Quant for a homogeneous distribution of radiotracer throughout a relatively large (~7 L) volume is good and comparable to that of PET (*1,13*).

Scanner variability and reconstruction parameters have been considered technologic factors affecting the accuracy of quantitative measurements in PET studies (*19,20*). The reproducibility of SPECT quantitation in the present study was good regardless of variability in imaging parameters. This good result might be associated with the cylindric phantom.

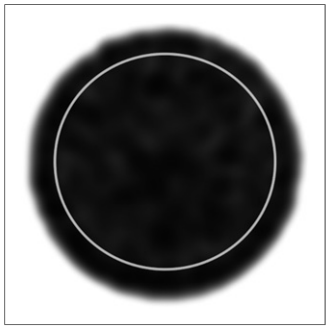

FIGURE 1. Representative slice of cylindric phantom. Gray circle indicates placement of region of interest on phantom.

TABLE 3
Radioactivity Concentrations in SPECT Images Under 2 Conditions at Participating Institutions

Institution	Radioactivity concentrations in SPECT images (kBq/mL)	
	Standardized conditions	Clinical conditions
A	99.65 ± 0.24	102.29 ± 0.55
B	99.32 ± 0.40	99.90 ± 0.25
C	101.33 ± 0.36	103.77 ± 0.51
D	102.96 ± 0.37	104.09 ± 0.24
E	108.35 ± 0.36	108.49 ± 0.11
F	95.71 ± 0.60	96.78 ± 0.64

TABLE 4
Radioactivity Concentrations in SPECT Images in Repetitive Experiment at Institution A

Scanner	Radioactivity concentrations in SPECT images (kBq/mL)		
	Test 1	Test 2	Test 3
1	98.96 ± 0.07	100.58 ± 0.86	100.01 ± 0.51
2	99.65 ± 0.24	101.53 ± 0.22	101.81 ± 0.30

We selected this phantom to avoid errors due to the technical difficulties involved in phantom preparation at the participating institutions. One study that used a body phantom with spheric inserts found a larger variation in quantitative values for small spheres (*21*). The large object size and the difference in photon energy and count-rate from other radiotracers are the major limitations in this study, since absolute measurements are often of most interest when applied to much smaller foci of radiotracer uptake and are of special interest for the dosimetry of therapy agents (*22*). Because partial-volume effects are influenced by imaging conditions (*23–25*), the quantitative accuracy of xSPECT Quant requires further evaluation for smaller regions of interest that might be representative of focal uptake in a lesion, for example. Moreover, previous studies mentioned that the quantitative values might be influenced by the noise characteristics in the xSPECT Bone algorithm (*26*,*27*). xSPECT Bone incorporated a weighted correction according to zone classification based on CT data. Our study design did not assess the effect of tissues zones used during reconstruction, and the 3.89% variation in clinical protocols that we found between institutions does not address the effect of zoning during reconstruction.

Dose calibrator accuracy and scanner calibration are also considerable factors in quantitative measurements (*19*,*20*). Because the filled radioactivity in the phantom was measured with each institution's own dose calibrator, dose calibrator bias had to be considered. A comparison of Tables 3 and 5 shows that the measurement accuracy of each institution's dose calibrator had a direct impact on bias in the radioactivity concentration in SPECT images. For example, because the dose calibrator at institution E was shown to underestimate the radioactivity, compared with the value calibrated by the manufacturer, a higher radioactivity might have been used in the cylinder phantom prepared at this site. In short, the interinstitutional variation in the phantom study can be attributed mainly to the variability in dose calibrator accuracy at the participating sites. This attribution is strengthened by the excellent intrainstitutional repeatability at institution A, as tested with identical dose calibrators. In addition to intrinsic factors such as device calibration and electronic response, the radioactivity measurement of the dose calibrator depends on source shape, material, volume, and surroundings (*28–31*). Each institution in our study used a commercially available ^{99m}Tc source with the same lot number to minimize variables. However, slight individual differences cannot be denied. Our study showed some general differences in measurement of radioactivity among the 6 institutions, including differences in manipulation (e.g., shielding with lead material) and in environment (e.g., temperature and humidity), not only in the intrinsic error of the devices.

TABLE 5
Measurement Accuracy for Each Institutional Dose Calibrator

Institution	Dose calibrator	Accuracy (%)
A	IGC-7E	1.68 ± 0.42
B	IGC-7	1.95 ± 0.76
C	CRC-55tW	1.82 ± 0.69
D	IGC-7	4.54 ± 0.39
E	ATOMLAB 500	−4.90 ± 0.21
F	IGC-7F	6.13 ± 0.44

Lack of a common source for calibrating detector sensitivity created potential for variability in our study. Miyaji et al. reported that the SCF of the ^{99m}Tc source depended on the preparation method whereas calibration using the ^{57}Co standard source was stable over a long period (*32*). Anizan et al. also mentioned that precise preparation and careful measurement of the calibration-source activity and acquisition on a background of negligible radiation are required for stable planar-sensitivity–based calibration (*33*). The effects of differences among calibration sources were not assessed in this study; hence, we have no details about variability.

Although the types of dose calibrators, calibration sources, and other items differed among the participating institutions, the reproducibility of SPECT quantitation was sufficient to discuss quantitative uptake equally among multiple centers. Our results indicated that xSPECT Quant harmonizes variability in a multicenter setting. However, the present phantom measurements were limited to a single radioactivity concentration, and only 1 measurement was conducted at each institute. The interinstitutional variability and accuracy of SPECT quantitation await future evaluation.

CONCLUSION

A commercially available quantitative SPECT application reproduced radioactivity concentrations with an interinstitutional variation of 4.2%, which is comparable to the variation for PET in a comparatively large (~7 L), homogeneous object. This multicenter study was the first step toward verification of SPECT quantitation, and further investigation of accuracy is desirable. Nonetheless, our findings are significant in terms of clinical assessments of SUV using SPECT/CT.

DISCLOSURE

No potential conflict of interest relevant to this article was reported.

ACKNOWLEDGMENT

We thank Nihon Medi-Physics Co., Ltd., for technical support. We also thank Takeshi Shimizu (Siemens Healthcare K.K.) for assistance.

REFERENCES

1. Bailey DL, Willowson KP. Quantitative SPECT/CT: SPECT joins PET as a quantitative imaging modality. *Eur J Nucl Med Mol Imaging.* 2014;41(suppl):S17–S25.
2. Jansen FP, Vanderheyden JL. The future of SPECT in a time of PET. *Nucl Med Biol.* 2007;34:733–735.
3. Madsen MT. Recent advances in SPECT imaging. *J Nucl Med.* 2007;48:661–673.
4. Rahmim A, Zaidi H. PET versus SPECT: strengths, limitations and challenges. *Nucl Med Commun.* 2008;29:193–207.
5. Ritt P, Vija H, Hornegger J, Kuwert T. Absolute quantification in SPECT. *Eur J Nucl Med Mol Imaging.* 2011;38(suppl):S69–S77.
6. Zeintl J, Vija AH, Yahil A, Hornegger J, Kuwert T. Quantitative accuracy of clinical ^{99m}Tc SPECT/CT using ordered-subset expectation maximization with 3-dimensional resolution recovery, attenuation, and scatter correction. *J Nucl Med.* 2010;51:921–928.
7. Cachovan M, Vija AH, Hornegger J, Kuwert T. Quantification of ^{99m}Tc-DPD concentration in the lumbar spine with SPECT/CT. *EJNMMI Res.* 2013;3:45.
8. Beck M, Sanders JC, Ritt P, Reinfelder J, Kuwert T. Longitudinal analysis of bone metabolism using SPECT/CT and ^{99m}Tc-diphosphonopropanedicarboxylic acid: comparison of visual and quantitative analysis. *EJNMMI Res.* 2016;6:60.
9. Hippeläinen E, Tenhunen M, Mäenpää H, Sohlberg A. Quantitative accuracy of ^{177}Lu SPECT reconstruction using different compensation methods: phantom and patient studies. *EJNMMI Res.* 2016;6:16.
10. Lee H, Kim JH, Kang YK, Moon JH, So Y, Lee WW. Quantitative single-photon emission computed tomography/computed tomography for technetium pertechnetate thyroid uptake measurement. *Medicine (Baltimore).* 2016;95:e4170.
11. Seret A, Nguyen D, Bernard C. Quantitative capabilities of four state-of-the-art SPECT-CT cameras. *EJNMMI Res.* 2012;2:45.
12. Dewaraja YK, Frey EC, Sgouros G, et al. MIRD pamphlet no. 23: quantitative SPECT for patient-specific 3-dimensional dosimetry in internal radionuclide therapy. *J Nucl Med.* 2012;53:1310–1325.
13. Bailey DL, Willowson KP. An evidence-based review of quantitative SPECT imaging and potential clinical applications. *J Nucl Med.* 2013;54:83–89.
14. Vija AH. Introduction to xSPECT technology: evolving multi-modal SPECT to become context-based and quantitative. In: Vija AH, ed. *Molecular Imaging White Paper.* Siemens Medical Solutions USA, Inc., Molecular Imaging; 2014.
15. Ma J, Vija AH. Evaluation of quantitation accuracy for xSPECT. In: *Nuclear Science Symposium and Medical Imaging Conference (NSS/MIC).* IEEE; 2015: 1–4.
16. Kuji I, Yamane T, Seto A, Yasumizu Y, Shirotake S, Oyama M. Skeletal standardized uptake values obtained by quantitative SPECT/CT as an osteoblastic biomarker for the discrimination of active bone metastasis in prostate cancer. *Eur J Hybrid Imaging.* 2017;1:2.
17. Armstrong IS, Hoffmann SA. Activity concentration measurements using a conjugate gradient (Siemens xSPECT) reconstruction algorithm in SPECT/CT. *Nucl Med Commun.* 2016;37:1212–1217.
18. Scheuermann JS, Saffer JR, Karp JS, Levering AM, Siegel BA. Qualification of PET scanners for use in multicenter cancer clinical trials: the American College of Radiology Imaging Network experience. *J Nucl Med.* 2009;50:1187–1193.
19. Boellaard R. Standards for PET image acquisition and quantitative data analysis. *J Nucl Med.* 2009;50(suppl):11S–20S.
20. Adams MC, Turkington TG, Wilson JM, Wong TZ. A systematic review of the factors affecting accuracy of SUV measurements. *AJR.* 2010;195:310–320.
21. Kangasmaa TS, Constable C, Hippeläinen E, Sohlberg AO. Multicenter evaluation of single-photon emission computed tomography quantification with third-party reconstruction software. *Nucl Med Commun.* 2016;37:983–987.
22. Kennedy JA, Lugassi R, Gill R, Keidar Z. Digital solid-state SPECT/CT quantitation of absolute ^{177}Lu-radiotracer concentration: in vivo/in vitro validation. *J Nucl Med.* 2020;61:1381–1387.
23. Knoll P, Kotalova D, Köchle G, et al. Comparison of advanced iterative reconstruction methods for SPECT/CT. *Z Med Phys.* 2012;22:58–69.
24. Soret M, Bacharach SL, Buvat I. Partial-volume effect in PET tumor imaging. *J Nucl Med.* 2007;48:932–945.
25. Onishi H, Motomura N, Fujino K, Natsume T, Haramoto Y. Quantitative performance of advanced resolution recovery strategies on SPECT images: evaluation with use of digital phantom models. *Radiol Phys Technol.* 2013;6:42–53.
26. Okuda K, Fujii S, Sakimoto S. Impact of novel incorporation of CT-based segment mapping into a conjugated gradient algorithm on bone SPECT imaging: fundamental characteristics of a context-specific reconstruction method. *Asia Ocean J Nucl Med Biol.* 2019;7:49–57.
27. Miyaji N, Miwa K, Tokiwa A, et al. Phantom and clinical evaluation of bone SPECT/CT image reconstruction with xSPECT algorithm. *EJNMMI Res.* 2020;10:71.
28. Bergeron DE, Cessna JT, Golas DB, Young RK, Zimmerman BE. Dose calibrator manufacturer-dependent bias in assays of ^{123}I. *Appl Radiat Isot.* 2014; 90:79–83.
29. Santos JAM, Carrasco MF, Lencart J, Bastos AL. Syringe shape and positioning relative to efficiency volume inside dose calibrators and its role in nuclear medicine quality assurance programs. *Appl Radiat Isot.* 2009;67:1104–1109.
30. Calhoun JM, Golas DB, Harris SG. Effects of varying geometry on dose calibrator response: cobalt-57 and technetium-99m. *J Nucl Med.* 1987;28:1478–1483.
31. Jacobson AF, Centofanti R, Babalola OI, Dean B. Survey of the performance of commercial dose calibrators for measurement of ^{123}I activity. *J Nucl Med Technol.* 2011;39:302–306.
32. Miyaji N, Miwa K, Motegi K, et al. Validation of cross-calibration schemes for quantitative bone SPECT/CT using different sources under various geometric conditions. *Nihon Hoshasen Gijutsu Gakkai Zasshi.*2017;73:443–450.
33. Anizan N, Wang H, Zhou XC, Hobbs RF, Wahl RL, Frey EC. Factors affecting the stability and repeatability of gamma camera calibration for quantitative imaging applications based on a retrospective review of clinical data. *EJNMMI Res.* 2014;4:67.